Oscillation of Capacitance inside Nanopores

ARTICLE *in* NANO LETTERS · DECEMBER 2011

Impact Factor: 13.59 · DOI: 10.1021/nl202952d · Source: PubMed

3 AUTHORS:

De-en Jiang
University of California, Riverside
151 PUBLICATIONS **4,902** CITATIONS
SEE PROFILE

Zhehui Jin
Reservoir Engineering Research Institute
18 PUBLICATIONS **333** CITATIONS
SEE PROFILE

Jianzhong Wu
University of California, Riverside
155 PUBLICATIONS **4,323** CITATIONS
SEE PROFILE

NANO LETTERS

LETTER

pubs.acs.org/NanoLett

Oscillation of Capacitance inside Nanopores

De-en Jiang,*,† Zhehui Jin,‡ and Jianzhong Wu*,‡

†Chemical Sciences Division, Oak Ridge National Laboratory, Oak Ridge, Tennessee 37831, United States

‡Department of Chemical and Environmental Engineering, University of California, Riverside, California 92521, United States

Supporting Information

ABSTRACT: Porous carbons of high surface area are promising as cost-effective electrode materials for supercapacitors. Although great attention has been given to the anomalous increase of the capacitance as the pore size approaches the ionic dimensions, there remains a lack of full comprehension of the size dependence of the capacitance in nanopores. Here we predict from a classical density functional theory that the capacitance of an ionic-liquid electrolyte inside a nanopore oscillates with a decaying envelope as the pore size increases. The oscillatory behavior can be attributed to the interference of the overlapping electric double layers (EDLs); namely, the maxima in capacitance appear when superposition of the two EDLs is most constructive. The theoretical prediction agrees well with the experiment when the pore size is less than twice the ionic diameter. Confirmation of the entire oscillatory spectrum invites future experiments with a precise control of the pore size from micro- to mesoscales.

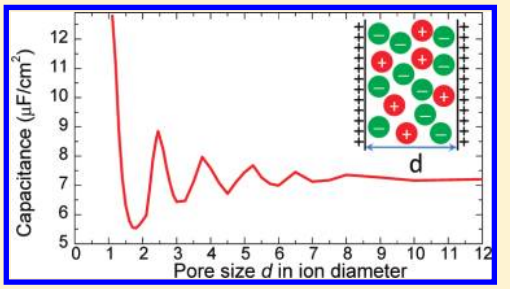

KEYWORDS: Supercapacitors, capacitance oscillation, electric double layers, ionic liquids, interference, density functional theory

Electric energy storage becomes increasingly imperative as more electricity is generated from renewable sources such as solar and wind at remote areas. Supercapacitors (also known as electric double layer capacitors or ultracapacitors) have the advantages of high power density, fast charging/discharging cycles (within seconds), and extremely long cycle life.[1,2] These advantages make supercapacitors attractive for broad applications such as in memory backup power and in the gasoline/electric hybrid bus.[3]

Carbon materials are promising as cost-effective electrode materials for supercapacitors.[4] Beyond the traditional activated carbons,[5] new forms such as carbide-derived carbons,[6,7] graphene,[2,8] and carbon onions[9] have been used for supercapacitors that display distinct characteristics such as ultrathin form[8] and ultrahigh power.[9] An interesting observation that has attracted great attention recently is the "anomalous" increase of the capacitance as the pore size approaches the electrolyte−ion dimensions.[6] This anomalous increase is observed not only in the traditional electrolyte such as tetraethylammonium tetrafluoroborate in acetonitrile (TEA-BF_4/ACN)[6] but also in ionic liquid 1-ethyl-3-methylimidazolium bis(trifluoromethylsulfonyl) imide (EMIM-TFSI).[10] The pore-size dependence of capacitance has been explained in terms of desolvation in the case of the traditional electrolyte[11−13] and image forces that exponentially screen the electrostatic interaction among ions within the narrow pore.[14−16] Atomistic molecular dynamics simulation of a supercapacitor made of an ionic liquid confined inside a nanotube also showed the increase in capacitance as the diameter of the tube decreases to the ion size.[17] However, it remains unclear how the capacitance changes with the pore size in the intermediate pore-size range (that is, from one to multiple times the electrolyte−ion diameters). Understanding the dependence of the capacitance on the pore size for these mesosclaes would facilitate developing mesoporous and hierarchical porous carbons for supercapacitors.[18−20]

Recently, Centeno et al.[21] measured the capacitances of 28 carbon electrodes of very different average pore sizes, ranging from 0.7 to 15 nm. They found that the surface-area normalized capacitance randomly fluctuates around a relatively constant value; they did not observe the anomalous increase of capacitance.[21] The disagreement with the previous experiments[6,10] has profound implication for practical applications of supercapacitors and thus calls for a deeper understanding of the size dependence of the capacitance in the micropore (<2 nm) to mesopore (2−50 nm) ranges where one expects overlapping of electric double layers.

In this Letter, the classical density functional theory (DFT)[22] is employed to examine the capacitance of an ionic liquid inside nanopores and its responses to the pore size and the ionic distributions. As demonstrated in previous works,[23,24] classical DFT provides an ideal tool to interrogate the overlapping EDLs and the capacitance behavior. It can reproduce the behavior of the differential capacitance of an ionic liquid at a planar electrode[23] from an analytical theory.[25] In comparison to alternate theoretical methods, DFT is computationally efficient and allows one to precisely tune the external parameters such as ion diameter and pore size over a large range of length scales.

Our theoretical investigation is based on the restricted primitive model for ionic liquids: both cations and anions are represented by hard spheres of the same diameter (σ = 0.5 nm) but

Received: August 24, 2011
Revised: October 11, 2011
Published: October 26, 2011

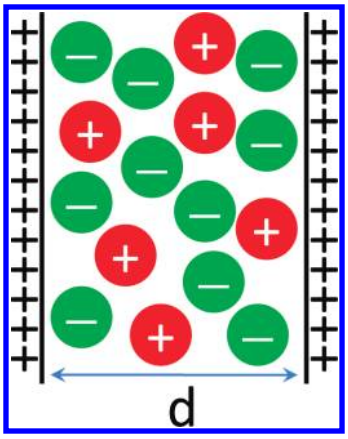

Figure 1. The restricted primitive model of an ionic liquid inside a slit pore. The pore width, designated as d, is defined as the surface to surface distance between two symmetric walls that have the same surface charge density.

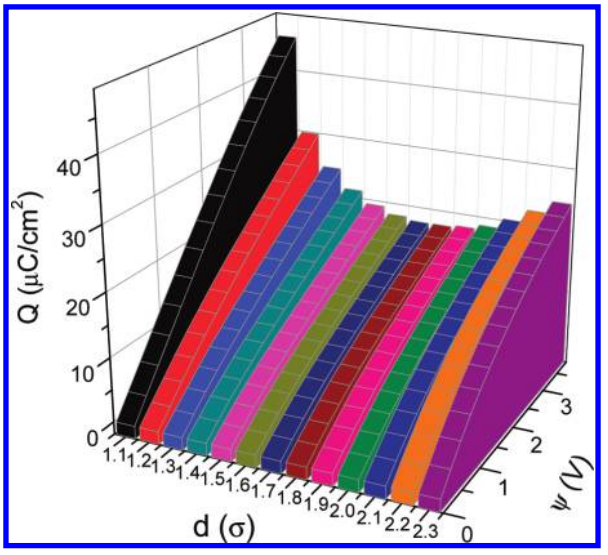

Figure 2. Surface charge density (Q) vs surface potential (ψ) and pore size (d). Here σ = 0.5 nm.

opposite charge (valence $Z = \pm 1$); the porous electrode is represented by a slit consisting of two symmetric hard walls of equal surface charge density (Figure 1). Approximately, the ion diameter corresponds to the averaged dimension of EMIM and TFSI ions used in the experiment.[10] Moreover, we chose our model ionic liquid to have the molar volume of EMIM-TFSI (259 cm^3/mol at 298 K and 1 bar). The two pore walls are separated by d, the surface-to-surface distance. For a given d, we vary the surface potential (ψ) and solve for the distributions of cations and anions from the DFT. On the basis of the density profiles, we obtain the surface charge density (Q) and the mean electrostatic potential across the pore (see the Supporting Information for computational details). Each pore configuration yields a plot of ψ versus Q; by varying d, we arrive at a series of Q vs ψ plots (Figure 2).

Figure 2 shows the dependence of surface charge density Q with respect to surface potential ψ as the pore size d varies from 1.1 to 2.3σ incrementally. Here the pore size d is expressed in terms of the ion diameter (σ = 0.5 nm). One can see that the surface charge density increases dramatically when the pore size approaches the ion diameter (that is, d decreases toward 1). In other words, at the same surface potential more charges are stored when d approaches the ion diameter.

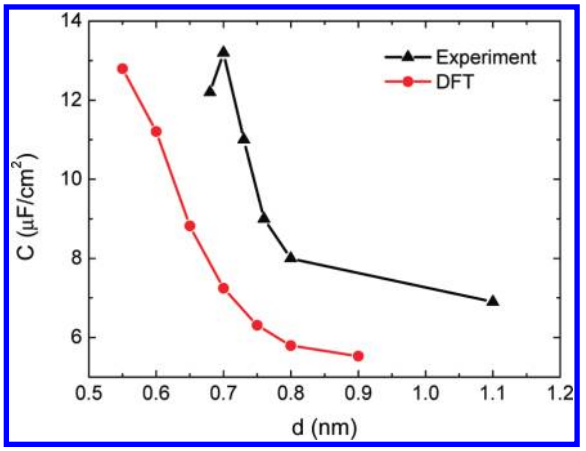

Figure 3. Capacitance of a nanoporous electrode as a function of the pore size, in comparison with the experiment.[10]

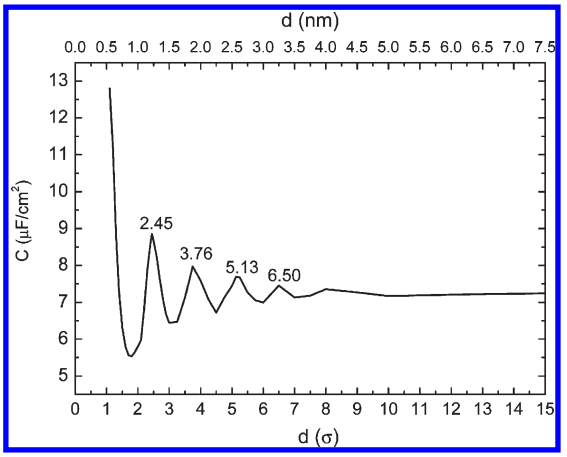

Figure 4. Capacitance (C) of a nanoporous electrode as a function of the pore width (d) up to 15σ. Peak positions are labeled in terms of the ion diameter (σ = 0.5 nm).

The capacitance (C) of the nanoporous electrode is defined as the charge to potential ratio at the surface, that is, $C = Q/\psi$. Figure 3 shows C as a function of d when the surface potential is fixed at 1.5 V; the results are similar at other surface potentials. For comparison, the experimental results of the EMIM-TFSI ionic liquid inside a nanopore of carbide-derived carbon is also plotted.[10] While the two curves appear horizontally shifted in part due to our approximate models for the EMIM-TFSI ionic liquid and the pore, it is clear that the DFT prediction matches very well the experimental results[10] in terms of (1) the rapid increase of the capacitance as the pore size decreases, (2) the magnitude of the increase (about two times), and (3) the maximum value of the capacitance (about 13 $\mu F/cm^2$). The rapid increase of the capacitance in small pores can be attributed to the denser packing of counterions and exclusion of the co-ions as the pore size is comparable to the ion diameter. Although earlier studies suggested such an effect arising from the image forces,[14−16] explicit consideration of the ion size and the electrostatic interactions appears

dx.doi.org/10.1021/nl202952d |Nano Lett. 2011, 11, 5373–5377

sufficient to reproduce the experimental results. Because the dielectric constant of a carbon material[26] is very close to that of an ionic liquid,[27] we expect that here the image charge effect should be insignificant for the capacitance dependence on the pore size. Atomistic MD simulation[17] was also able to show the rapid increase in capacitance without image forces, albeit the magnitude of the simulated capacitance had to be scaled 9 times to match the experimental values.

A closer examination of Figure 2 reveals that at the same surface potential, the surface charge and thus the capacitance increases as the pore size increases from 1.7 to 2.3σ. The obvious question here is what would happen if the pore size increases further. To address this question, we performed more DFT calculations to obtain Q versus ψ plots for d up to 15σ (7.5 nm). Figure 4 shows the capacitance as a function of the pore size. The DFT predicts that the capacitance oscillates as the pore size increases and that the multiple peaks (corresponding to pore sizes of d = 2.45, 3.76, 5.18, and 6.50σ) exhibit a decaying envelope similar to that for the interaction potential between two parallel surfaces.[28] Apparently, the "anomalous" increase of capacitance at the ion-dimension pore size[6,10] is only part of the picture (that is, d from 1.6 to 1.0σ). Because the pore size used in our theoretical calculation has a resolution of 0.1σ (~0.05 nm) for the multiple peaks to manifest themselves, experimental validation of the full capacitance spectrum would require a challenging pore size control. This requirement has two implications: (1) the pore-size change needs to be "digitally" tuned to give a progressive spacing of 0.1−0.2σ; (2) for a specific pore size, the pore-size distribution should be as narrow as possible and ideally within 0.2σ (~0.1 nm). The previous success with pore-size control of carbide-derived carbons[29] suggests that at least the first predicted peak at 2.45σ may be validated.

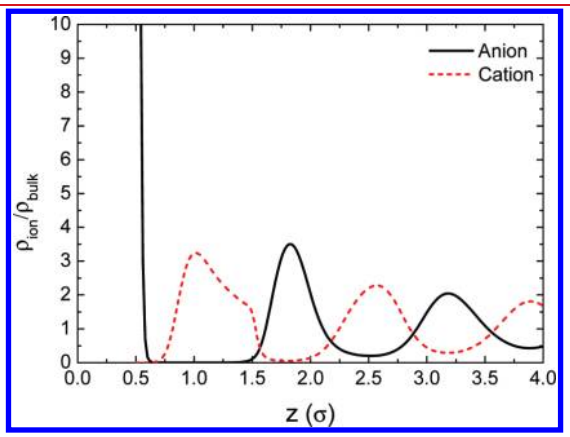

Figure 5. Density profiles of cations and anions near one charged wall as a function of the distance from the wall (z).

The capacitance profile shown in Figure 4 provides a reconciliation of the apparent conflict between the "anomalous" increase[6,10] reported for carbide-derived carbons and the "regular pattern" reported for a variety of porous carbons.[21] Namely, the constant value from the regular pattern reported by Centeno et al.[21] involves very different porous carbons which may have a rather large pore size distribution. As shown in Figure 4, a precise control of the pore size is needed to see both the "anomalous" increase and the oscillatory profile. A broad distribution of pore size is likely to yield a random relationship of capacitance versus pore size around a constant value, as seen in the experimental data by Centeno et al.[21]

What are the causes of the capacitance oscillation? In these pore sizes of 1−10 times the ion diameter (Figure 4), one expects significant overlap of electric double layers (EDLs) from the two charged walls, especially for ionic liquids which tend to form multiple alternating layers of cations and anions at the electrode.[30−34] Intuitively, one may consider the overlapping of EDLs as superimposing of two standing waves on each other. Indeed, the peak positions in Figure 4 coincide with constructive superposition of the ionic density profiles in the EDLs as explained in the following.

Let us first consider the ionic density profiles near a single charged wall. Figure 5 shows the density profiles of the cations and anions near an isolated surface with a potential of 1.5 V. Different from that of a typical EDL in aqueous solutions, the structure of an ionic liquid EDL shows alternating layers of cations and anions extending far away from the charged wall. Now imagine that two such layered structures are overlapped near two symmetric walls opposite to each other. Figure 6 shows the density profiles assuming that the two layered structures were independent of each other. Here the pore width is d = 2.45σ, corresponding to the first peak position in Figure 4. One can see that at this pore size there is significant "resonance" of the ionic density for the same charged ion from both walls. Because of such "resonance", the ionic density profiles inside the pore (Figure 7) reflect a constructive superposition of the EDLs, reminiscent of interference in wave propagation. We find similar interference pattern at the other peak positions (d = 3.76, 5.13, and 6.5σ; see Figures S1−S3 in the Supporting Information).

The equal-sized hard spheres used in this work to model the cation and anion of an IL are simple, in comparison with the

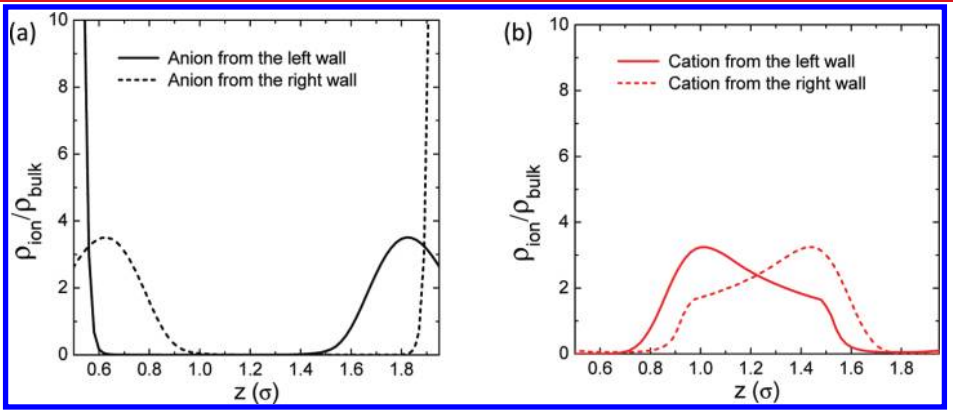

Figure 6. The superimposed density profiles of anions (a) and cations (b) in a slit pore of width d = 2.45σ. Here we assume that the EDLs are noninteracting, that is, the ionic density profiles can be superimposed. The left wall is at z = 0; the right wall at z = 2.45σ. The surface potential is at 1.5 V.

dx.doi.org/10.1021/nl202952d |Nano Lett. 2011, 11, 5373–5377

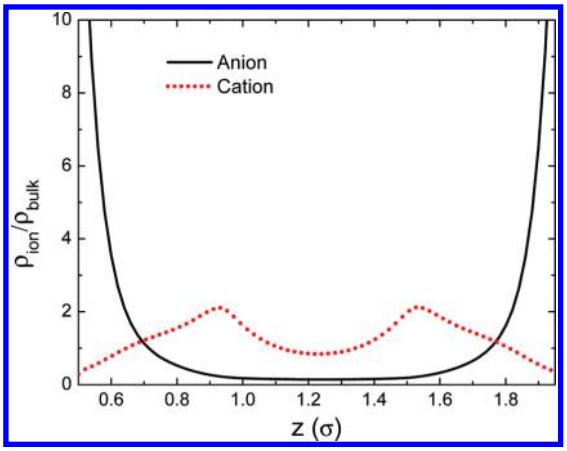

Figure 7. The real density profiles of anions and cations. All conditions are the same as those discussed in Figure 6.

complex molecular shapes of the real ILs such as EMIM-TFSI. But the beauty of the classical DFT method is its simplicity which allows one to capture the most essential physics with the simplest models. Nevertheless, it would be more desirable to consider more sophisticated molecular models. Recently, we have examined the effect of adding a neutral tail to the cation sphere and found that the EDL structure at a planar electrode does not change too much from that of the simple hard-sphere models.[35] This suggests that the capacitance oscillation inside the nanopore is likely to be seen also in more complex models for the IL. We are pursuing this idea for the future work. Moreover, we hope that more sophisticated modeling such as all-atom molecular dynamics simulations can further confirm our prediction of the capacitance oscillation and its explanation in terms of the interference of the IL EDL structure.

As we argued above, experimental confirmation of our prediction requires precise control of pore size. Besides carbide derived carbons, we think that another promising material bridging the micro-to-meso pore range is conductive porous frameworks which have narrow pore-size distributions. Here we note a very recent paper on supercapactive energy storage using an aza-fused π-conjugated microporous framework;[36] as a nitrogen-doped π-system, this type of material is not expected to be a good electrical conductor.[37] Since our prediction was based on the assumption that the electrode is not a good electrical conductor (as we did not include the image charge in our model system), the π-conjugated frameworks might be better suited for confirming our prediction of capacitance oscillation if one could synthesize them with progressive pore sizes.

In summary, we have studied the size dependence of capacitance for an ionic liquid inside slit pores using a classical density functional theory. We predicted oscillation of the capacitance as a function of the pore size resembling that for interaction potential between two charged surfaces. As the pore size increases from one to many times the ion diameter, the capacitance shows multiple peaks with a decaying envelope. The peak capacitance appears when the electric double layers (EDLs) from the two walls have the most constructive interference; that is, the density of one ion from one pore wall overlaps or resonates most with that of the same-charged ion from the other wall. Although the calculation is focused on ionic liquids inside a nanopore, we expect that a similar trend may hold for a conventional electrolyte such as tetraethylammonium tetrafluoroborate in acetonitrile. The present work implies that the pore size of carbon materials needs to be precisely controlled to achieve optimal capacitance.

■ ASSOCIATED CONTENT

Supporting Information. Details of the density functional theory method employed and superimposed density profiles of anions and cations in slit pores of width $d = 3.76\sigma$, 5.13σ, and 6.50σ, assuming that the EDLs are noninteracting. This material is available free of charge via the Internet at http://pubs.acs.org/.

■ AUTHOR INFORMATION

Corresponding Author
*E-mail: jiangd@ornl.gov and jwu@engr.ucr.edu.

■ ACKNOWLEDGMENT

D.J. was supported as part of the Fluid Interface Reactions, Structures, and Transport (FIRST) Center, an Energy Frontier Research Center funded by the U.S. Department of Energy, Office of Science, Office of Basic Energy Sciences under Award No. ERKCC61 (D.J.). Additional support (J.W.) is provided by the National Science Foundation (NSF-CBET-0852353). This research also used resources of the National Energy Research Scientific Computing Center, which is supported by the Office of Science of the U.S. Department of Energy under Contract No. DE-AC02-05CH11231.

■ REFERENCES

(1) Simon, P.; Gogotsi, Y. *Nat. Mater.* **2008**, *7*, 845.
(2) Miller, J. R.; Outlaw, R. A.; Holloway, B. C. *Science* **2010**, *329*, 1637.
(3) Miller, J. R.; Simon, P. *Science* **2008**, *321*, 651.
(4) Pandolfo, A. G.; Hollenkamp, A. F. *J. Power Sources* **2006**, *157*, 11.
(5) Gamby, J.; Taberna, P. L.; Simon, P.; Fauvarque, J. F.; Chesneau, M. *J. Power Sources* **2001**, *101*, 109.
(6) Chmiola, J.; Yushin, G.; Gogotsi, Y.; Portet, C.; Simon, P.; Taberna, P. L. *Science* **2006**, *313*, 1760.
(7) Chmiola, J.; Largeot, C.; Taberna, P. L.; Simon, P.; Gogotsi, Y. *Science* **2010**, *328*, 480.
(8) Yoo, J. J.; Balakrishnan, K.; Huang, J.; Meunier, V.; Sumpter, B. G.; Srivastava, A.; Conway, M.; Mohana Reddy, A. L.; Yu, J.; Vajtai, R.; Ajayan, P. M. *Nano Lett.* **2011**, *11*, 1423.
(9) Pech, D.; Brunet, M.; Durou, H.; Huang, P. H.; Mochalin, V.; Gogotsi, Y.; Taberna, P. L.; Simon, P. *Nat. Nanotechnol* **2010**, *5*, 651.
(10) Largeot, C.; Portet, C.; Chmiola, J.; Taberna, P. L.; Gogotsi, Y.; Simon, P. *J. Am. Chem. Soc.* **2008**, *130*, 2730.
(11) Chmiola, J.; Largeot, C.; Taberna, P. L.; Simon, P.; Gogotsi, Y. *Angew. Chem., Int. Ed.* **2008**, *47*, 3392.
(12) Huang, J. S.; Sumpter, B. G.; Meunier, V. *Angew. Chem., Int. Ed.* **2008**, *47*, 520.
(13) Huang, J. S.; Sumpter, B. G.; Meunier, V. *Chem.—Eur. J.* **2008**, *14*, 6614.
(14) Kondrat, S.; Kornyshev, A. *J. Phys.—Condes. Matter* **2011**, *23*, 022201.
(15) Kondrat, S.; Georgi, N.; Fedorov, M. V.; Kornyshev, A. A. *Phys. Chem. Chem. Phys.* **2011**, *13*, 11359.
(16) Skinner, B.; Chen, T. R.; Loth, M. S.; Shklovskii, B. I. *Phys. Rev. E* **2011**, *83*, 056102.
(17) Shim, Y.; Kim, H. J. *ACS Nano* **2010**, *4*, 2345.
(18) Vix-Guterl, C.; Frackowiak, E.; Jurewicz, K.; Friebe, M.; Parmentier, J.; Beguin, F. *Carbon* **2005**, *43*, 1293.
(19) Xing, W.; Qiao, S. Z.; Ding, R. G.; Li, F.; Lu, G. Q.; Yan, Z. F.; Cheng, H. M. *Carbon* **2006**, *44*, 216.

(20) Wang, D. W.; Li, F.; Liu, M.; Lu, G. Q.; Cheng, H. M. *Angew. Chem., Int. Ed.* **2008**, *47*, 373.
(21) Centeno, T. A.; Sereda, O.; Stoeckli, F. *Phys. Chem. Chem. Phys.* **2011**, *13*, 12403.
(22) Wu, J. Z.; Li, Z. D. *Annu. Rev. Phys. Chem.* **2007**, *58*, 85.
(23) Jiang, D. E.; Meng, D.; Wu, J. Z. *Chem. Phys. Lett.* **2011**, *504*, 153.
(24) Forsman, J.; Woodward, C. E.; Trulsson, M. *J. Phys. Chem. B* **2011**, *115*, 4606.
(25) Kornyshev, A. A. *J. Phys. Chem. B* **2007**, *111*, 5545.
(26) Taft, E. A.; Philipp, H. R. *Phys. Rev.* **1965**, *138*, A197.
(27) Min, Y. J.; Akbulut, M.; Sangoro, J. R.; Kremer, F.; Prud'homme, R. K.; Israelachvili, J. *J. Phys. Chem. C* **2009**, *113*, 16445.
(28) Israelachvili, J. N. *Intermolecular and Surface Forces*, 2nd ed.; Academic Press: London, 1992.
(29) Presser, V.; Heon, M.; Gogotsi, Y. *Adv. Funct. Mater.* **2011**, *21*, 810.
(30) Fedorov, M. V.; Kornyshev, A. A. *Electrochim. Acta* **2008**, *53*, 6835.
(31) Yang, L.; Fishbine, B. H.; Migliori, A.; Pratt, L. R. *J. Am. Chem. Soc.* **2009**, *131*, 12373.
(32) Wang, S.; Li, S.; Cao, Z.; Yan, T. Y. *J. Phys. Chem. C* **2010**, *114*, 990.
(33) Vatamanu, J.; Borodin, O.; Smith, G. D. *J. Am. Chem. Soc.* **2010**, *132*, 14825.
(34) Feng, G.; Qiao, R.; Huang, J. S.; Dai, S.; Sumpter, B. G.; Meunier, V. *Phys. Chem. Chem. Phys.* **2011**, *13*, 1152.
(35) Wu, J. Z.; Jiang, T.; Jiang, D. E.; Jin, Z. H.; Henderson, D. *Soft Matter* **2011**, DOI: 10.1039/c1sm06089a.
(36) Kou, Y.; Xu, Y.; Guo, Z.; Jiang, D. *Angew. Chem., Int. Ed.* **2011**, *50*, 8753.
(37) Zhang, Y.; Mori, T.; Ye, J.; Antonietti, M. *J. Am. Chem. Soc.* **2010**, *132*, 6294.